In Vitro Cellular & Developmental Biology - Animal (2021) 57:539–549
https://doi.org/10.1007/s11626-021-00578-2

Cultivation of fractionated cells from a bioactive-alkaloid-bearing marine sponge *Axinella* sp.

Yuefan Song[1,2] · Yi Qu[3] · Xupeng Cao[4] · Wei Zhang[5] · Fuming Zhang[2] · Robert J. Linhardt[2] · Qi Yang[6]

Received: 23 December 2020 / Accepted: 5 April 2021 / Published online: 4 May 2021 / Editor: Tetsuji Okamoto

Abstract
Sponges are among the most primitive multicellular organisms and well-known as a major source of marine natural products. Cultivation of sponge cells has long been an attractive topic due to the prominent evolutionary and cytological significance of sponges and as a potential approach to supply sponge-derived compounds. Sponge cell culture is carried out through culturing organized cell aggregates called 'primmorphs.' Most research culturing sponge cells has used unfractionated cells to develop primmorphs. In the current study, a tropical marine sponge *Axinella* sp., which contains the bioactive alkaloids, debromohymenialdisine (DBH), and hymenialdisine (HD), was used to obtain fractionated cells and the corresponding primmorphs. These alkaloids, DBH and HD, reportedly show pharmacological activities for treating osteoarthritis and Alzheimer's disease. Three different cell fractions were obtained, including enriched spherulous cells, large mesohyl cells, and small epithelial cells. These cell fractions were cultivated separately, forming aggregates that later developed into different kinds of primmorphs. The three kinds of primmorphs obtained were compared as regards to appearance, morphogenesis, and cellular composition. Additionally, the amount of alkaloid in the primmorphs-culture system was examined over a 30-d culturing period. During the culturing of enriched spherulous cells and developed primmorphs, the total amount of alkaloid declined notably. In addition, the speculation of alkaloid secretion and some phenomena that occurred during cell culturing are discussed.

Keywords Sponge · Cell culture · Primmorphs · Cell separation · Bioactive alkaloids

Introduction

Known as the most primitive invertebrates, sponges are sessile filter feeders that lack true tissues throughout their bodies. The physiological functions of these organisms are performed through cooperation of different cell types specialized for distinct functions. The sponge cells can be roughly categorized into epithelial cells and mesohyl cells (Funayama 2018). One type of epithelial cells is pinacocytes that serve as epidermal cells, lining the outermost portion of the sponge body and part

✉ Yuefan Song
syf@dlou.edu.cn; songyuefan421@gmail.com

Yi Qu
qyi0656@gmail.com

Xupeng Cao
c_x_p@dicp.ac.cn

Wei Zhang
wei.zhang@flinders.edu.au

Fuming Zhang
zhangf2@rpi.edu

Robert J. Linhardt
linhar@rpi.edu

Qi Yang
qi.yang@flinders.edu.au

[1] College of Food Science and Engineering, Key Laboratory of Aquatic Product Processing and Utilization of Liaoning Province, Dalian Ocean University, Dalian, China

[2] Center for Biotechnology and Interdisciplinary Studies, Rensselaer Polytechnic Institute, Troy, NY, USA

[3] Dalian Environmental Monitoring Center, Dalian, China

[4] State Key Laboratory of Catalysis, Dalian Institute of Chemical Physics, Chinese Academy of Sciences, Dalian, China

[5] Centre for Marine Bioproducts Development, College of Medicine and Public Health, Flinders University, Adelaide, South Australia, Australia

[6] Center for Marine Drugs, State Key Laboratory of Oncogene and Related Genes, Department of Pharmacy, Renji Hospital, School of Medicine, Shanghai Jiao Tong University, Shanghai, China

of the interior canal system. Another type of epithelial cells is choanocytes (also known as 'collar cells') constituting the choanocyte chambers and lining the canal system together with pinacocytes. The beating of the flagella from choanocytes creates directed water current through the sponge, bringing in food particles that are trapped by the 'collar' cilia of choanocytes and are taken up by phagocytosis. The remainder of the sponge body enclosed by epithelial cells is called the mesohyl, a jelly-like substance containing collagens, skeletal materials, and a variety of mesohyl cells. The category of mesohyl cells includes archaeocytes (the "stem cells" of sponges), sclerocytes (producing spicules, skeletal materials), collagen-expressing cells, spherulous cells (filled with distinctive inclusions), and some other minor types of cells (Ereskovsky 2010; Simpson 2012). The major approach to identify sponge cell types is generally made through microscopic observation of cellular morphology, although in some cases cellular identification through examination of molecular markers seem to be promising (Funayama *et al.* 2005a; Funayama *et al.* 2005b; Funayama 2018).

In addition to the different types of sponge cells, there are also various symbiotic microorganisms that abundantly reside within sponges (Hentschel *et al.* 2006). Sponges have long been known to be a remarkable resource for mining novel microbial strains (Fuerst 2014). Due to their sessile filter-feeding lifestyle (requiring the development of chemical defense systems against predators, pathogens, and competitors) and their rich content of symbiotic microorganisms, sponges are now the most prolific source of marine natural products (Carroll *et al.* 2020). The pharmaceutical development of novel sponge-derived compounds requires a large, reliable source of biomaterial. However, it is not feasible to solve the supply problem through the massive harvesting of wild sponges, which would be environmentally detrimental (Grasela *et al.* 2012). Since only a few sponge-derived molecules are now available through chemical synthesis (Sipkema *et al.* 2005) and microbial fermentation (Leal *et al.* 2014), the amplification of sponge biomass is considered a promising strategy to solve the supply problem (Lanna *et al.* 2018). The attempts to expand sponge biomass are carried out through cultivation of sponge explants (Singh and Thakur 2015; Padiglia *et al.* 2018); Gökalp *et al.* 2019, buds (Rocher *et al.* 2020), larva (Borisenko *et al.* 2019), and dissociated cells (Cai and Zhang 2014). Sea-based culture of explants have proven to be feasible for a couple of sponge products (Sipkema *et al.* 2005; Carballo *et al.* 2010; Ruiz *et al.* 2013; Leal *et al.* 2014;), but approaches that are more efficient and widely-adapted for biomass multiplication have not yet been developed.

Cell culture is highlighted because of its potential to provide a controlled production in a defined system to scale up the production of sponge biomass. Marine sponge cells have a distinctive feature that they aggregate spontaneously when inoculated into Ca^{2+} /Mg^{2+} containing seawater (Wilson 1907). The aggregates, usually initially loose and irregular, later develop into compact spherical bodies covered by a smooth layer of pinacocytes. The aggregates at this stage are called 'primmorphs' and characterized by the formation of continuous pinacoderm (Custodio *et al.* 1998). So far, cell culture techniques for marine sponges are built almost totally based on the primmorphs model, which are able to maintain the production of bioactive metabolites during culture (Müller *et al.* 2000; Rady *et al.* 2016; Rady *et al.* 2019). Although there are currently no sponge cell lines available, even after 2 decades of exploration, recent research reported encouraging results on cultures of three sponge species that were subcultured from 3 to 5 times, with an average of 5.99 population doublings after subculturing when using an optimized nutrient medium (Conkling *et al.* 2019). In addition to efforts at improving cell culture techniques (Schippers *et al.* 2011; Pozzolini *et al.* 2014; Huete-Stauffer *et al.* 2015; Munroe *et al.* 2019), primmorphs have also been used as models to study spiculogenesis (Annenkov and Danilovtseva 2016; Danilovtseva *et al.* 2019; Markl *et al.* 2020), cryopreservation (Mussino *et al.* 2013), cellular aggregation and adhesion (Vilanova *et al.* 2010; Vilanova *et al.* 2020), morphogenesis and development (Eerkes-Medrano *et al.* 2015; Ereskovsky *et al.* 2016; Lavrov and Kosevich 2016; Lavrov *et al.* 2020), the relationships between sponge cells and microbes (Chernogor *et al.* 2020), and aquatic pollution monitoring (Akpiri *et al.* 2017; Akpiri *et al.* 2020).

In our previous study (Song *et al.* 2011), we discovered two alkaloids, debromohymenialdisine (DBH) and hymenialdisine (HD), from a tropical sponge *Axinella* sp. We identified four major types of cells, including the large mesohyl cells, the epithelial cells, and two types of spherulous cells. Through a cell-separation protocol, we successfully obtained the enriched cell fractions, and localized the two alkaloids DBH and HD in the spherulous cells. In the current study, we employed a simplified cell-separation procedure to acquire three cell fractions and cultivated these separately to obtain three different aggregates (A1, A2, and A3), which later developed into different primmorphs. To the best of our knowledge, the present work is the first to describe the development of different primmorphs from different cell types. To date, there are only a few reports describing primmorphs generated from enriched archaeocytes (Zhang *et al.* 2003; Sun *et al.* 2007). The majority of primmorph research has been carried out using unfractionated cells. The cultivation of fractionated cells from bioactive-alkaloids-bearing sponge described in this paper provides insights into the morphogenetic features of different primmorphs, as well as variations in alkaloid contents during the culture period. In addition, some observations made in these culturing experiments allow speculation on the secretion pathway of the alkaloids and discovery of the cellular traits and functions of different sponge cell types.

Materials and methods

Marine sponge *Axinella sp.* *Axinella* sp. was collected from the South China Sea (Qu *et al.* 2012) and packaged in plastic bags filled with seawater. After arriving in the lab, the sponges were kept in aquaria with running seawater at 25°C prior to use.

Reagents Calcium-/magnesium-free artificial seawater (CMFASW) and CMFASW containing ethylenediaminetetraacetic acid (EDTA) (CMFASW-E) were prepared as described by Song *et al.* (2011). CMFASW contained 35.00 g NaCl, 0.99 g Na_2SO_4, 0.75 g KCl, and 2.42 g Tris-base in 1 L water, and the final pH was adjusted using HCl solution to 8.0. CMFASW-E contained 25.0 mM EDTA in addition to the CMFASW ingredients. CMFASW, CMFASW-E, and natural seawater (NSW) were sterilized at 110°C for 15min.

Cell fractionation and culture The sponge specimens were dissociated as described as previous reported (Song *et al.* 2011). Briefly, the samples were cleaned with CMFASW, sliced (2–3 mm thick), and soaked in CMFASW-E for 15min. The slices were gently squeezed with tweezers to release cells. The resultant cell suspensions were filtered through a 48-μm nylon mesh to remove spicules and debris. The cell suspension was then placed in Petri dishes (100 mm, Corning, Glendale, AZ) for 30 min, during which time the spherulous cells spontaneously agglomerate in CMFASW-E. The dishes were then shaken 5–10 s to re-suspend all the cell contents. The spherulous-cell clusters resettled fast to the Petri dish bottom while the single cells remained in suspension. The single cell suspension was then pipetted out and subjected to centrifugation at 29×*g* for 10min, and the subsequent supernatant was further centrifuged at 110×*g* for 10min. At the end, the cell pellets from 29×*g* and 110×*g* centrifugation, along with the spherulous-cell clusters, were separately inoculated into 6-well plates filled with NSW (containing 400mg/L gentamicin) at a final density of 2, 4, and 1.8×10^6 cells/mL, respectively. The cells were cultured at 24°C, and the media were replaced every 1–4 d. All the replaced media were collected for alkaloid quantification. The aggregates/pellets formed by enriched spherulous cells were named as A1. The aggregates formed by cell fraction collected from 29×*g* centrifugation (mainly consisted of large or dense cells from mesohyl, such as archaeocytes and unagglomerated spherulous cells) were named A2. The aggregates formed by cell fraction collected from 110×*g* centrifugation (mainly epithelial cells that are smaller than mesohyl cells, including choanocytes and pinacocytes) were named A3. The preparation procedures for aggregates A1–A3 from sponge specimens are illustrated in Fig. 1.

Hematoxylin-eosin (HE) staining Cell aggregates A1–A3 were fixed in 10% formalin for 8–15h, dehydrated with ethanol and embedded in paraffin, sectioned using microtome (Shandon, Altrincham, UK), and stained (Leica Autostainer XL, Wetzlar, Germany) with hematoxylin and eosin. The histological sections were observed using light microscope (Nikon TE2000, Tokyo, Japan) equipped with a DS-U2 digital camera.

Microscopic observation The morphologies of A1, A2, and A3 were observed and recorded during culture using light microscopy (Nikon TE2000, Tokyo, Japan). The aggregates were also dissociated using CMFASW-E at the 5, 10, 15, and 20^{th} day after inoculation. The cell suspension (20 μL) was spread on a slide and observed under microscopic vision. Proportions of different kinds of cells were calculated by counting more than 400 cells from at least five visual fields.

Quantification of DBH and HD alkaloids Quantification of alkaloids in A1–A3 and culture media was carried out through measuring the absorbance of the cellular extracts and replaced media at 350nm using a UV-visible spectrophotometer (Jasco, UV/VIS V-530, Tokyo, Japan). This is a convenient and fast approach well adapted to salty samples (i.e., NSW culture media), which is a risk for an HPLC system without a proper pretreatment. DBH and HD are two major secondary metabolites in *Axinella* sp., which can be identified from the total-ion-chromatogram spectra (Fig. A1) using UPLC/Q-TOF MS (Waters, Milford, MA). The UPLC spectra of sponge specimen scanned at different UV wavelengths showed a specific peak at 350nm for DBH and HD (Fig. A2) suggesting UV absorbance at 350nm is primarily attributed to DBH and HD. Therefore, the absorbance at 350 nm directly corresponds to the total amount of DBH and HD in samples. The molar absorption coefficients for DBH and HD (20.6 and 17.8×10^{-3} L/ (mol . cm), respectively, were determined to establish a formula using UV absorbance to calculate the amount of alkaloid (Fig. A3). Using an HPLC method, we quantified DBH and HD in 12 specimens (including sponge bodies, different kinds of primmorphs, and cell fractions) from 5 sponge individuals and found that in all specimens, the relative amount of DBH and HD was stable (the value was 2.3:1, Fig. A4). Based on the above results, the following formula was established: A (absorbance at 350nm) =M (the total molar concentration of alkaloids, mM) × (20.6×2.3 + 17.8 ×1)/(2.3+1), which can be simplified as M (the total molar concentration of alkaloids, mM) =0.05 A (absorbance at 350nm) (1).

The cell and media samples were collected in days 0, 5, 10, 15, 20, 25, and 30, freeze-dried, weighed, and followed with methanol extraction of alkaloid products. The extracts were dried in a fume hood in dark, dissolved in dimethylsulfoxide (DMSO), diluted with an equal volume of methanol, and examined the absorbance at 350nm. The replaced media were collected and centrifuged at 20,000×*g* for 10 min. The resulting supernatant was directly examined at 350nm. The pellet was extracted with 2 mL of methanol, centrifuged again,

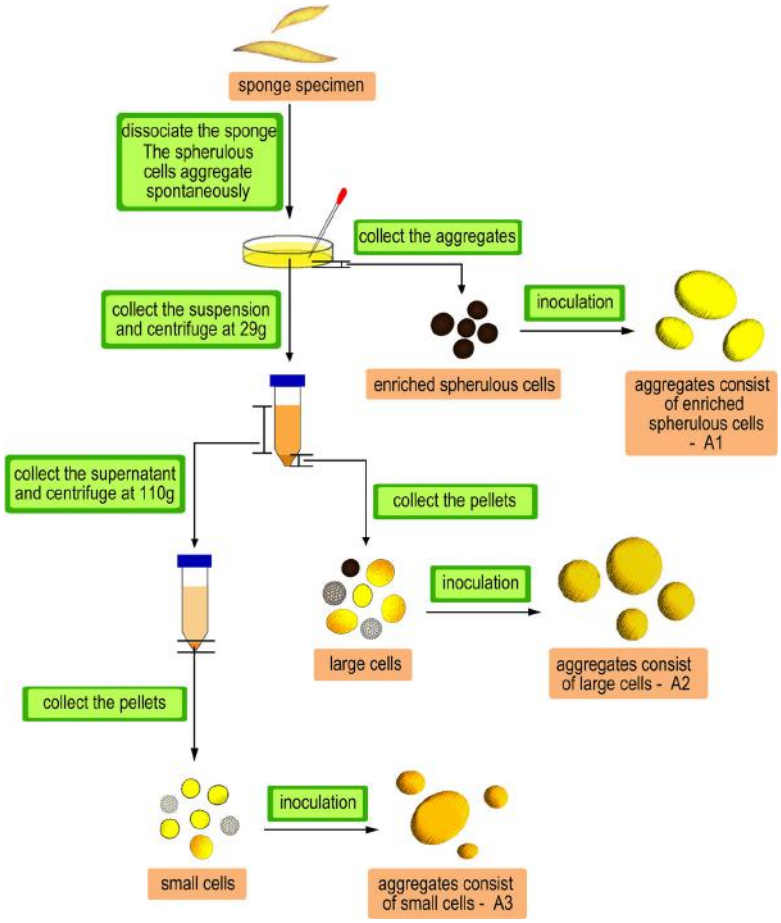

Figure 1. Protocol for preparation of aggregates A1–A3 using fractionated cells from *Axinella* sp.

and the methanol supernatant was subjected to detection at 350nm. The total alkaloid amount in each sample was derived using calculated concentration (from Formula (1)).

Results

The overall features of A1–A3 primmorphs The A1–A3 primmorphs showed different features in appearance and inner structure. All the three kinds of primmorphs had distinctive colors. The spherulous-cell-enriched primmorphs (A1 primmorphs) exhibited a bright yellow appearance, while A2 and A3 were earth yellow and orange, respectively (Fig. 2*a, c, e*). Our previous work had found that the spherulous cells of *Axinella* sp. were eosinophilic. The results of HE staining showed a coincidence in that A1, which mainly consists of spherulous cells, was primarily pink due to being eosinophilic (Fig. 2*b*). In the A2 primmorphs, the outer part is hematoxylinophilic, and the eosinophilic spherulous cells gathered into pink clusters scattered in the inner parts of the pellets (Fig. 2*d*). A3 was hematoxylinophilic, suggesting that it has a high capacity for proliferation (Fig. 2*f*).

Morphogenesis of A1–A3 The fractionated cells aggregated immediately after inoculation and turned into pellets with smooth surfaces within 4–8 d. At the beginning, all the three kinds of aggregates appeared to be loose (Fig. 3*a, d, g*). Broken cells were excluded during the formation of primmorphs. It took 3–4 d for A1 to reshape and another 3–4 d to produce a smooth epithelium (Fig. 3*b*). A2 and A3 quickly formed into a regular spherical shape and generated a smooth surface within 96 h after inoculation. A3 was inclined to attach on the bottom of the plate as early as day 8 but was disturbed by replacement of culture medium. A3 finally tightly adhered to the bottom of the plate on day 14 and gradually spread like a sponge explant. A2 started to adhere since day 18. A1 showed no tendency to attach to the bottom of the plate during the 30 d of cultivation.

Cellular compositions of A1–A3 A1–A3 were sampled and dissociated at different times during the culture period (Fig. 4). The dissociated cells were classified into four categories for counting and analysis (Fig. 5). The spherulous cells, exhibiting a dark appearance under light microscopy, were counted separately, and all other cells, with relatively clear

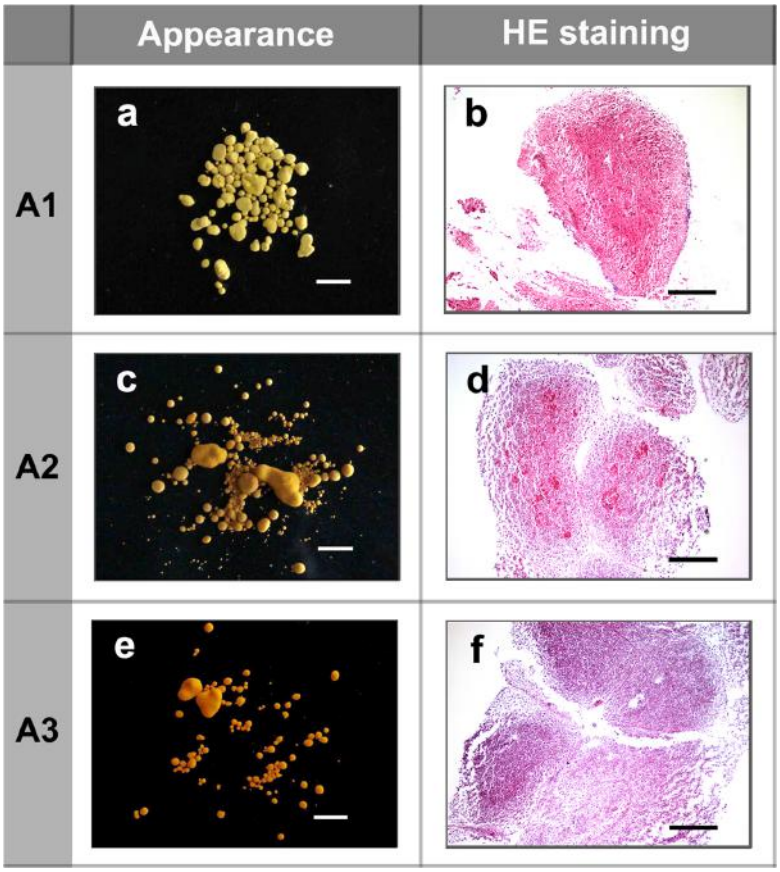

Figure 2. Images of morphologies and hematoxylin-eosin (HE) staining of A1–A3 primmorphs on day 8. *a*, *c*, *e* the morphologies of A1 (*a*), A2 (*c*) and A3 (*e*), *bar*=5mm; *b*, *d*, *f*, light microscopy images of HE staining of A1 (*b*), A2 (*d*) and A3 (*f*), *bar*=500μm.

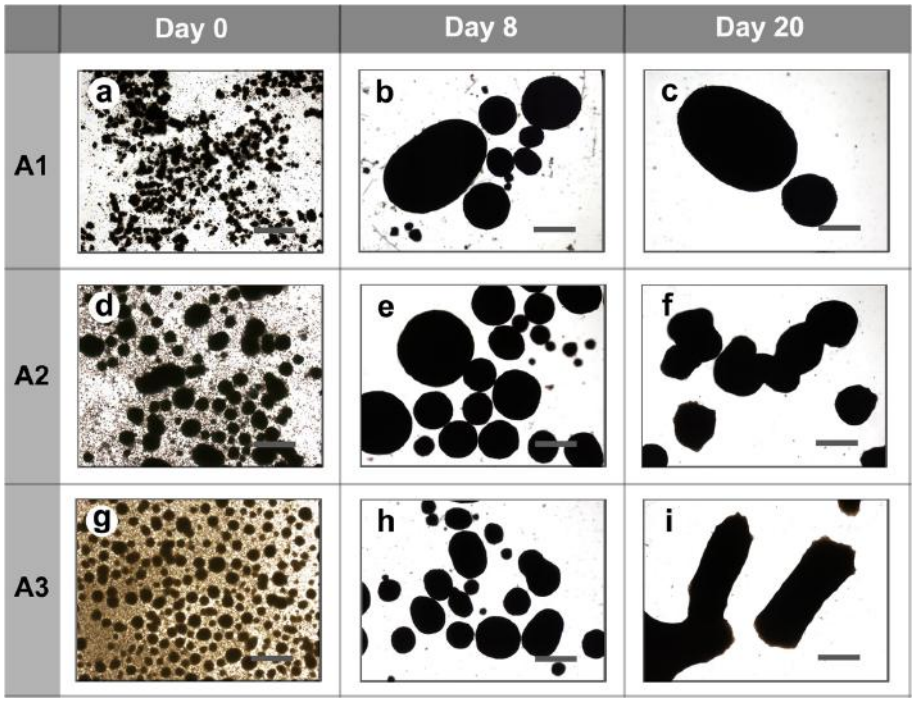

Figure 3. Morphology of A1–A3 observed using light microscope. *a*, A1, day 0; *b*, A1, day 8; *c*, A1, day 20; *d*, A2, day 0; *e*, A2, day 8; *f*, A2, day 20; *g*, A3, day 0; *h*, A3, day 8; *i*, A3, day 20. *Bar*=50μm.

cytoplasm, were classified by size with a range of diameters (<10μm, 10–20μm, and >20μm). The cells of <10μm in diameter were mostly choanocytes and pinacocytes. Cells having a diameter between 10 and 20μm were mainly archaeocytes and other large mesohyl cells, and the cells >20μm in diameter might be phagocytes. The cellular compositions in A1, A2, and A3 varied similarly. The proportion of small cells (<10μm) declined, and the proportion of big cells (>10μm) increased in A1, A2, and A3. This pattern suggested that phagocytosis is a common phenomenon in all types of aggregates. Huge dark cells were observed under microscopy among the cells dissociated from A1 (Fig. 4*b, c, triangle*), as a result of spherulous cells being engulfed by archaeocytes or other phagocytic cells. The A3 showed a sharp decline in the proportion of small cells from day 0 to day 5, which was primarily caused by exclusion of dead cells from the aggregates during the first few days. The percentage of small cells in A3 also gradually declined from day 5 to day 20, likely caused by cell death and subsequent phagocytosis of the dead cells. The average cellular size in A3 remarkably increased during 20 d of incubation (Fig. 5*c*). A large population in A3 exhibited an archeocyte appearance under microscopy in the late stage of culturing (Fig. 4*i*).

Variation of alkaloid content in A1–A3 culture systems The alkaloid concentration in A1 remained stable in the first 5 d and markedly declined during day 5 to day 10 (Fig. 6*a*). From days 10 to 30 the concentration of compounds was maintained between 0.5 and 0.6 mmol/g (dry weight) in A1. The biomass of the aggregates also decreased. Some cells were excluded from the forming aggregates and caused a one-third loss in biomass in the first 5 d. Then the biomass of aggregates slowly declined from days 5 to 30. The alkaloid amount remaining in A1 was calculated using concentration multiplying by biomass (Fig. 6*c, grey*), fell sharply before day 10 and then decreased gradually until the end of culturing. The amount of alkaloid in replaced culture media was also examined. Most of the environmental alkaloid was dissolved in media, but a small portion remained in cell debris and needed to be extracted before analysis (Fig. 6*b*). The variation of alkaloid amount in an overall culture system was calculated by summing all alkaloid remaining in the aggregates (Fig. 6*c, grey*) with all that had been released into media (Fig. 6*c, pink*) in one well of the culture plate. From days 0 to 10, 20% of total alkaloid in the overall culture system vanished (Fig. 6*c*). This might be caused by oxidation or H_2O addition reaction of the environmental alkaloids, resulting in a reduction of absorbance at 350nm.

In the culture system of A2 and A3, the alkaloids content fluctuated similarly within 30 d (Fig. 6*d–i*). The concentration of alkaloid in aggregates was relatively stable while the biomass declined quickly within the first 5 d (Fig. 6*d, g*). In contrast to A1, there was no sharp decline in the concentration of alkaloid in A2 and A3 during days 5–10. Additionally, there was no net loss in total alkaloid in the A2 and A3 culture systems (Fig. 6*f, i*).

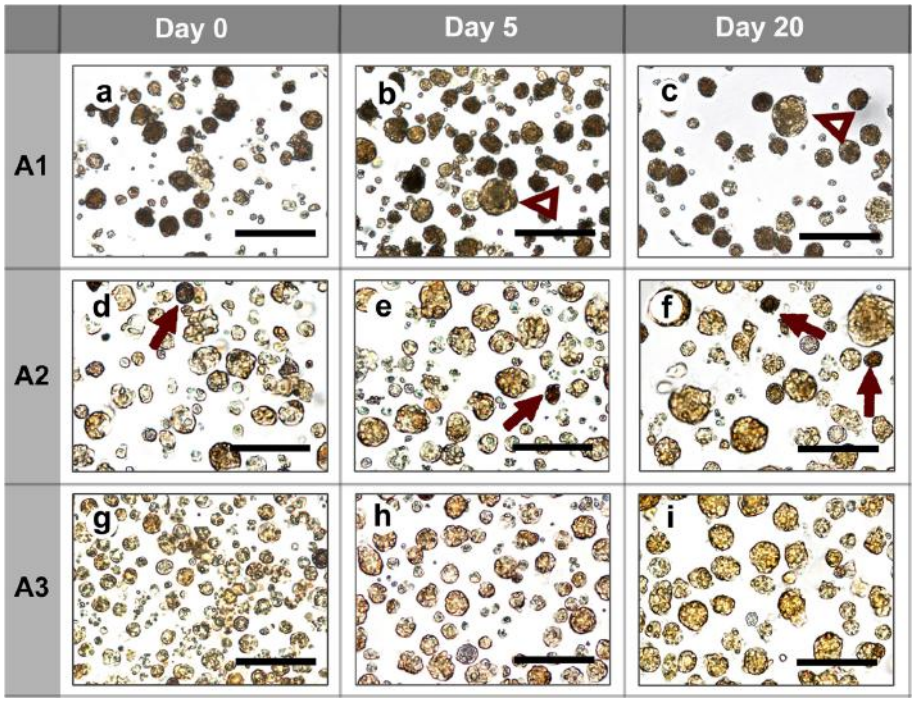

Figure 4. Dissociated cells from A1, A2, and A3. *a*, A1, day 0; *b*, A1, day 5; *c*, A1, day 20; *d*, A2, day 0; *e*, A2, day 5; *f*, A2, day 20; *g*, A3, day 0; *h*, A3, day 5; *i*, A3, day 20. *Hollow triangle*, huge cell with spherulous cells engulfed in; *arrow*, spherulous cells. *Bar*=50μm.

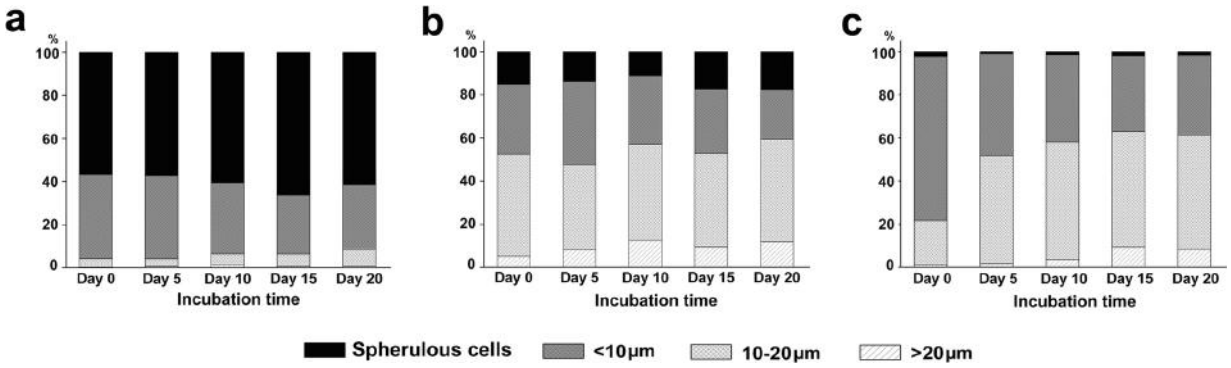

Figure 5. Proportions of different cells in A1, A2, and A3. Spherulous cells were identified according to their typical morphological features: dark color under light microscopy with a diameter range of 6–15 μm. The other cells were classified according to their diameters in size.

Discussion

The variation of alkaloid concentration in A1 primmorphs It can be learned from Fig. 6*f* to i that during the culturing of A2 and A3, the loss of alkaloid was generally in accordance with the loss of biomass, which mainly happened between days 0 and 5 as the dead cells were expelled during the formation of primmorphs. The concentration of alkaloid in A2 and A3 basically remained stable in the 30-d culture period (Fig. 6*d, g*). However, the concentration of alkaloid in A1 notably declined during days 5–10 (Fig. 6*a*), which was totally different from A2 to A3 but has been confirmed in multiple batches and repetitive experiments (data not shown). Also, we observed that during days 5–10, there were abundant particles with similar optical characteristics (dark brown under light microscopy) much smaller than spherulous cells appeared when A1 was dissociated (Fig. 7*a*). These kinds of particles were also found in the culture of unfractionated cells (not described in this article), commonly observed in the monolayer of the spreading edge when the primmorphs attached on the bottom of the Petri dish (Fig. 7*b*). TEM showed that they have similar intrastructure to the spherulous cells but were much smaller (Fig. 7*c, d*). Based on the above data, we speculated spherulous cells might secrete these particles. The particles containing DBH and HD may be discharged in the outer layer of sponge body or at the spreading edge of primmorphs to use against external hazards (i.e., predators and pathogens). Since these two compounds are inhibitors of cyclin-dependent kinases that are cytotoxic (therefore, they are isolated and stored in spherulous cells), the A1 may exclude certain amount of alkaloids during the formation of primmorphs (days 5–10, when a smooth epithelium was formed) to keep these compounds at an endurable level for the primmorphs to live and hence led to the marked decline of the alkaloids concentration in A1.

Some observations during the culture of fractionated cells Building a model system of culturing fractionated cells is not only informative in bioactive compound production but also provides many interesting phenomena that can be enlightening in exploring the cellular traits, functions, and differentiation relationships of sponge cells. Spicule production is quite commonly observed in sponge cell culture (Cao *et al.* 2007; Valisano *et al.* 2012). For *Axinella* sp., we observed sclerocytes producing spicules in primmorphs consisting of unfractionated cells after 2 wk of culturing (not described in this article, Fig. A5). However, in our experiment using fractionated cells, as described in this article, neither A1, A2, nor A3 produced any spicules within 30 d. This may be due to the incomplete function of A1/A2/A3 caused by lack of certain types of cells. Another possible explanation is primmorphs developed from fractionated cells which require more time (i.e., 2+ wk) to stably attach and extend on the bottom; hence, the associated morphogenesis is late, leading to the absence of spicule-forming during 30-d culture period.

Another observation is about cytochemical staining of spherulous cells. The spherulous cells from *Axinella* sp. contain special peroxisomes that are highlighted as dark particles when stained with DAB (3,3'-diaminobenzidine) (Fig. A6 *a*.,b). We used DAB to stain cells dissociated from A1–A3 primmorphs and found abundant positively stained small cells in A3 primmorphs cultured for 20 d (Fig. A6 *f*). Although the staining is diffusive in the cytoplasm and is different from the dark dots pattern in spherulous cells, there is also a suggestion that these cells found in A3 are probably undergoing differentiation into spherulous cells. However, this positively stained cell is relatively rare in archeocyte-predominated A2 primmorphs, which implicated us that compared to A2, the choanocyte-predominated A3 may have a higher potential for differentiating into spherulous cells.

Also, there is an interesting phenomenon about cell aggregation. Cell aggregation is universal in sponges. The intercellular adhesion and recognition in sponges

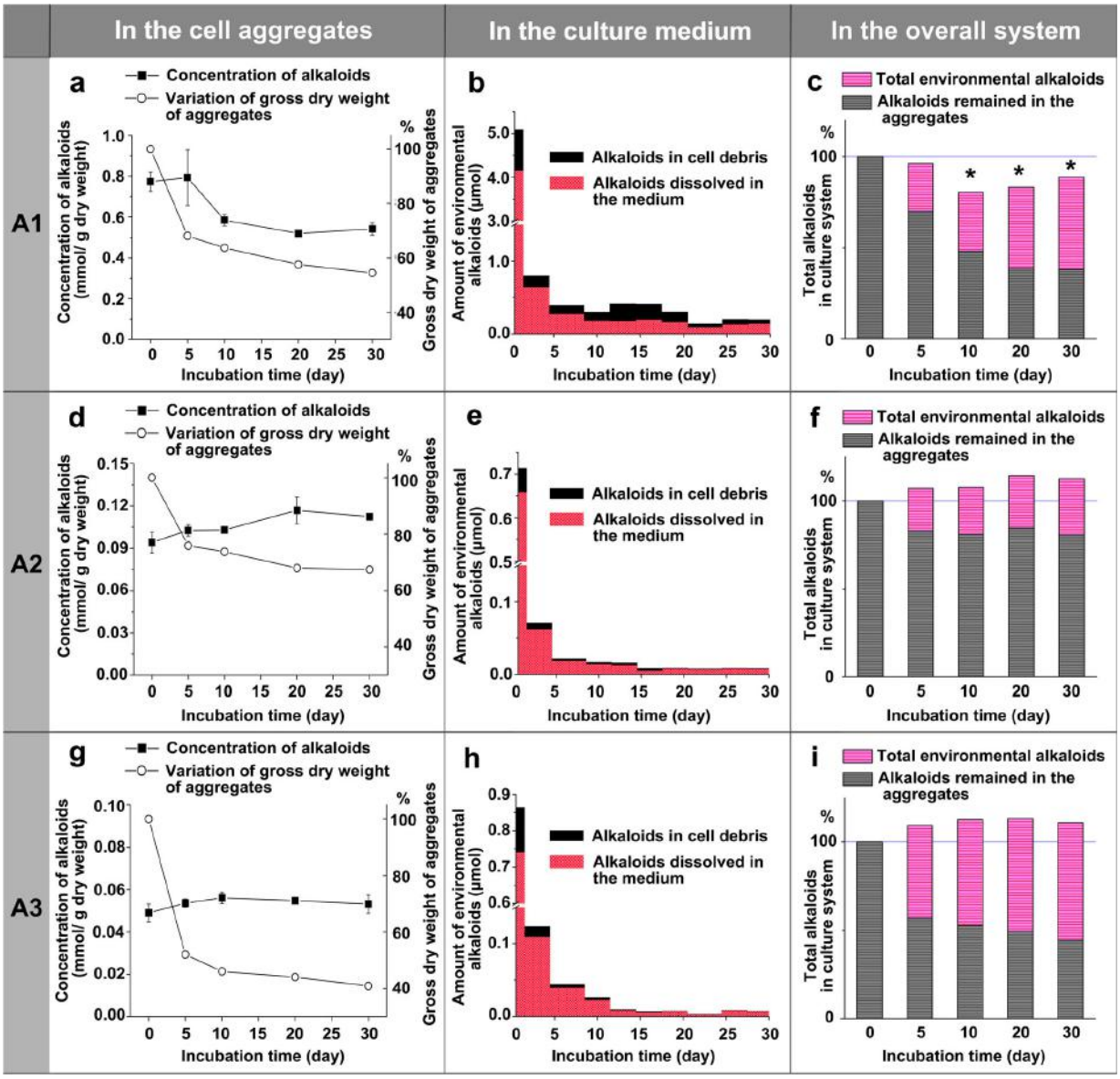

Figure 6. Alkaloid (total DBH and HD) content in cell aggregates, culture media, and the overall culture system of A1–A3. *Asterisk* is the significant difference at the level of $p<0.1$, *t*-test, and total alkaloids amount compared to that of day 0.

are mediated by proteoglycan-like molecules named aggregation factors (AFs). The sulfated glycans of AFs can achieve homophilic interaction through "calcium bridges" between their sulfate groups on glucose and fucose units (Vilanova *et al.* 2020). The marine sponge *Axinella* sp. is quite special in that the homotypic cells have a strong tendency to aggregate during dissociation in CFMASW-E. The spherulous cells, large mesohyl cells (such as archeocytes), and smaller epithelial cells (choanocytes and pinacocytes) tend to gather with homologous cells separately during dissociation (Fig. A7 *a*., *b*). We took advantage of this characteristic and developed a protocol to purify four different types of cells (Song *et al.* 2011). During the culture of A2 primmorphs, we noticed that the large mesohyl cells still aggregated with homologous cells after dissociation (Fig. A7 *c*., *arrow*). However, the spherulous cells (dark brown under light microscope) took part in the assembling with choanocytes/pinacocytes (Fig. A7 *d*) instead of gathering with other spherulous cells. This provided us an inspiration that the spherulous cells might have a close relationship to the choanocytes/pinacocytes in

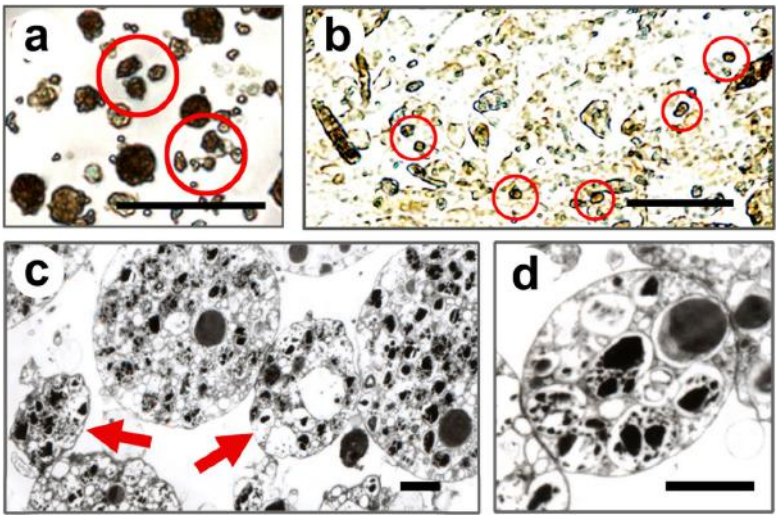

Figure 7. The spherulous-cell-like granules found in *Axinella* sp. ***a,*** the light microscopy image of granules in dissociated A1, *bar*=50μm; ***b,*** granules found during the culture of unfractionated cells (from another experiment not described in this article), *bar*=50μm; ***c***, ***d,*** TEM image of the granules, the *arrow* indicating granules next to spherulous cells, the granules (usually have a diameter <5 μm), and spherulous cells (diameter > 8 μm, usually) have similar condensed intrastructures which explain the dark brown appearance under light microscope—due to the reduced transmission of light, *bar*=2μm.

differentiation. It should be emphasized that the theories based on observations are highly speculative, and the "homologous" aggregation of cells from *Axinella* sp. was so far only determined using TEM (Song *et al.* 2011). Solid evidences from the molecular biology perspective are quite essential to further identify the exact cell types and to confirm the differentiation relationships among sponge cells (Adamska 2018; Funayama 2018; Musser *et al.* 2019; Peña *et al.* 2016).

Conclusions

In the present study, we carried out cell cultures using different cell fractions from *Axinella* sp. The spherulous-cell-enriched fraction formed irregular aggregates (A1) after inoculation and developed into primmorphs with smooth epithelium during days 6–8. A1 exhibited a bright yellow appearance and stayed unattached to the bottom of plates after 30 d. Another fraction consisting of large mesohyl cells (mainly including archaeocytes, sclerocytes, collagen-expressing cells, and some spherulous cells) quickly gathered into spherical aggregates (A2) after inoculation and generated a smooth epithelium within 4 days. A2 primmorphs were earth yellow in color, started to adhere on bottom after day 18 and extended in a limited fashion afterwards. The third fraction with small epithelial cells, pinacocytes and choanocytes, experienced a similar primmorphs-developing process to that of A2. The A3 primmorphs, thus formed, exhibited an orange color and remarkable adherent and spreading capacities. The proportions of large cells (diameter >10 μm) in A3 increased dramatically during the first 15 d, as a result of phagocytosis within the primmorphs. During the culture of A1, A2, and A3, a general and notable cell loss was found within the first 5 d as the dead cells were expelled during the formation of primmorphs. The alkaloid concentration basically remained stable in A2 and A3 primmorphs during culture, while markedly declining in A1 during days 5 to day 10. This decrease might result from the expulsion of alkaloid-containing particles from spherulous cells.

Supplementary Information The online version contains supplementary material available at https://doi.org/10.1007/s11626-021-00578-2.

Funding This research was funded by the China Scholarship Council (201908210162), the 'Hi-Tech Research and Development Program of China' (2006AA09Z435), and the National Natural Science Foundation of China (31801954).

References

Akpiri RU, Hodges NJ, Konya RS (2020) Aluminium induced DNA-damage and oxidative stress in cultures of the marine sponge Hymeniacidon perlevis. J Mar Sci. https://doi.org/10.30564/jms.v2i1.1070

Akpiri RU, Konya RS, Hodges NJ (2017) Development of cultures of the marine sponge Hymeniacidon perleve for genotoxicity assessment using the alkaline comet assay. Environ Toxicol Chem 36:3314–3323

Adamska M (2018) Differentiation and transdifferentiation of sponge cells. In Kloc M and Kubiak J (eds) Marine Organisms as Model Systems in Biology and Medicine. Springer, Cham, pp. 229–253. https://doi.org/10.1007/1978-1003-1319-92486-92481_92412

Annenkov VV, Danilovtseva EN (2016) Spiculogenesis in the siliceous sponge Lubomirskia baicalensis studied with fluorescent staining. J Struct Biol 194:29–37

Borisenko I, Podgornaya OI, Ereskovsky AV (2019) From traveler to homebody: Which signaling mechanisms sponge larvae use to become adult sponges? Adv Protein Chem Struct Biol. Elsevier:421–449

Cai X, Zhang Y (2014) Marine invertebrate cell culture: a decade of development. J Oceanogr 70:405–414

Cao X, Fu W, Yu X, Zhang W (2007) Dynamics of spicule production in the marine sponge Hymeniacidon perlevis during in vitro cell culture and seasonal development in the field. Cell Tissue Res 329: 595–608.

Carballo JL, Yañez B, Zubía E, Ortega MJ, Vega C (2010) Culture of explants from the sponge Mycale cecilia to obtain bioactive mycalazal-type metabolites. Mar Biotechnol 12:516–525

Carroll AR, Copp BR, Davis RA, Keyzers RA, Prinsep MR (2020) Marine natural products. Nat Prod Rep 37:175–223

Chernogor L, Klimenko E, Khanaev I, Belikov S (2020) Microbiome analysis of healthy and diseased sponges Lubomirskia baicalensis by using cell cultures of primmorphs. PeerJ 8:e9080

Conkling M, Hesp K, Munroe S, Sandoval K, Martens DE, Sipkema D, Wijffels RH, Pomponi SA (2019) Breakthrough in Marine invertebrate cell culture: sponge cells divide rapidly in improved nutrient Medium. Sci Rep 9:1–10

Custodio MR, Prokic I, Steffen R, Koziol C, Borojevic R, Brümmer F, Nickel M, Müller WE (1998) Primmorphs generated from dissociated cells of the sponge Suberites domuncula: a model system for studies of cell proliferation and cell death. Mech Ageing Dev 105: 45–59

Danilovtseva E, Pal'shin V, Zelinskiy S, Annenkov V (2019) Fluorescent dyes for the study of siliceous sponges. Limnology and Freshwater Biology:302–307

Eerkes-Medrano D, Feehan CJ, Leys SP (2015) Sponge cell aggregation: checkpoints in development indicate a high level of organismal complexity. Invertebr Biol 134:1–18

Ereskovsky AV (2010) The comparative embryology of sponges. Springer Science & Business Media;

Ereskovsky AV, Chernogor LI, Belikov SI (2016) Ultrastructural description of development and cell composition of primmorphs in the endemic Baikal sponge Lubomirskia baicalensis. Zoomorphology 135:1–17

Fuerst JA (2014) Diversity and biotechnological potential of microorganisms associated with marine sponges. Appl Microbiol Biotechnol 98:7331–7347

Funayama N (2018) The cellular and molecular bases of the sponge stem cell systems underlying reproduction, homeostasis and regeneration. Int J Dev Biol 62:513–525

Funayama N, Nakatsukasa M, Hayashi T, Agata K (2005a) Isolation of the choanocyte in the fresh water sponge, Ephydatia fluviatilis and its lineage marker, Ef annexin. Develop Growth Differ 47:243–253

Funayama N, Nakatsukasa M, Kuraku S, Takechi K, Dohi M, Iwabe N, Miyata T, Agata K (2005b) Isolation of Ef silicatein and Ef lectin as molecular markers sclerocytes and cells involved in innate immunity in the freshwater sponge Ephydatia fluviatilis. Zool Sci 22:1113–1122

Gökalp M, Wijgerde T, Sarà A, De Goeij JM, Osinga R (2019) Development of an integrated mariculture for the collagen-rich sponge Chondrosia reniformis. Mar Drugs 17:29. https://doi.org/10.3390/md17010029

Grasela JJ, Pomponi SA, Rinkevich B, Grima J (2012) Efforts to develop a cultured sponge cell line: revisiting an intractable problem. In Vitro Cellular & Developmental Biology-Animal 48:12–20

Hentschel U, Usher KM, Taylor MW (2006) Marine sponges as microbial fermenters. FEMS Microbiol Ecol 55:167–177

Huete-Stauffer C, Valisano L, Gaino E, Vezzulli L, Cerrano C (2015) Development of long-term primary cell aggregates from Mediterranean octocorals. In Vitro Cellular & Developmental Biology-Animal 51:815–826

Lanna E, Cajado B, Santos D, Cruz F, Oliveira F, Vasconcellos V (2018) Outlook on sponge reproduction science in the last ten years: are we far from where we should be? Invertebr Reprod Dev 62:133–142

Lavrov AI, Kosevich IA (2016) Sponge cell reaggregation: cellular structure and morphogenetic potencies of multicellular aggregates. J Exp Zool A Ecol Genet Physiol 325:158–177

Lavrov AI, Saidov DM, Bolshakov FV, Kosevich IA (2020) Intraspecific variability of cell reaggregation during reproduction cycle in sponges. Zoology:125795

Leal MC, Sheridan C, Osinga R, Dionísio G, Rocha RJM, Silva B, Rosa R, Calado R (2014) Marine microorganism-invertebrate assemblages: perspectives to solve the "supply problem" in the initial steps of drug discovery. Mar Drugs 12:3929–3952

Markl JS, Müller WE, Sereno D, Elkhooly TA, Kokkinopoulou M, Gardères J, Depoix F, Wiens M (2020) A synthetic biology approach for the fabrication of functional (fluorescent magnetic) bioorganic–inorganic hybrid materials in sponge primmorphs. Biotechnol Bioeng 117:1789–1804

Müller WE, Böhm M, Batel R, De Rosa S, Tommonaro G, Müller IM, Schröder HC (2000) Application of cell culture for the production of bioactive compounds from sponges: synthesis of avarol by primmorphs from Dysidea avara. J Nat Prod 63:1077–1081

Munroe S, Sandoval K, Martens DE, Sipkema D, Pomponi SA (2019) Genetic algorithm as an optimization tool for the development of sponge cell culture media. In Vitro Cellular & Developmental Biology-Animal 55:149–158

Musser JM, Schippers KJ, Nickel M, Mizzon G, Kohn AB, Pape C, Hammel JU, Wolf F, Liang C, Hernández-Plaza A (2019) Profiling cellular diversity in sponges informs animal cell type and nervous system evolution. BioRxiv:758276

Mussino F, Pozzolini M, Valisano L, Cerrano C, Benatti U, Giovine M (2013) Primmorphs cryopreservation: a new method for long-time storage of sponge cells. Mar Biotechnol 15:357–367

Padiglia A, Ledda FD, Padedda BM, Pronzato R, Manconi R (2018) Long-term experimental in situ farming of Crambe crambe (Demospongiae: Poecilosclerida). PeerJ 6:e4964

Peña JF, Alié A, Richter DJ, Wang L, Funayama N, Nichols SA (2016) Conserved expression of vertebrate microvillar gene homologs in choanocytes of freshwater sponges. EvoDevo 7:1–15

Pozzolini M, Mussino F, Cerrano C, Scarfì S, Giovine M (2014) Sponge cell cultivation: optimization of the model Petrosia ficiformis (Poiret 1789). J Exp Mar Biol Ecol 454:70–77

Qu Y, Song Y, Cao H, Zhang W (2012) Comparative study of morphological and molecular characters between two sponge specimens (Porifera: Demosponge: Axinella) with pharmacologically active compounds from the South China Sea. Pak J Zool 44:1727–1735

Rady H, Salem S, El-Arab ME (2019) Primmorph extracts and mesohyls of marine sponges inhibit proliferation and migration of hepatocellular carcinoma cells in vitro. Journal of pharmaceutical analysis 9: 284–291

Rady HM, Hassan AZ, Salem SM, Mohamed TK, Esmaiel NN, Ez-El-Arab MA, Ibrahim MA, Fouda FK (2016) Induction of apoptosis and cell cycle arrest by Negombata magnifica sponge in hepatocellular carcinoma. Med Chem Res 25:456–465

Rocher C, Vernale A, Fierro-Constain L, Sejourne N, Chenesseau S, Marschal C, Le Golf E, Dutilleul M, Matthews C, Marschal F (2020) The buds of Oscarella lobularis (Porifera): a new convenient model for sponge cell and developmental biology. bioRxiv. https://doi.org/10.1101/2020.06.23.167296

Ruiz C, Valderrama K, Zea S, Castellanos L (2013) Mariculture and natural production of the antitumoural (+)-discodermolide by the Caribbean marine sponge Discodermia dissoluta. Mar Biotechnol 15:571–583

Schippers KJ, Martens DE, Pomponi SA, Wijffels RH (2011) Cell cycle analysis of primary sponge cell cultures. In Vitro Cellular & Developmental Biology-Animal 47:302–311

Simpson TL (2012) The cell biology of sponges. Springer-Verlag; New York

Singh A, Thakur NL (2015) Field and laboratory investigations of budding in the tetillid sponge Cinachyrella cavernosa. Invertebr Biol 134:19–30

Sipkema D, Osinga R, Schatton W, Mendola D, Tramper J, Wijffels RH (2005) Large-scale production of pharmaceuticals by marine sponges: Sea, cell, or synthesis? Biotechnol Bioeng 90:201–222

Song Y-F, Qu Y, Cao X-P, Zhang W (2011) Cellular localization of debromohymenialdisine and hymenialdisine in the marine sponge Axinella sp. using a newly developed cell purification protocol. Mar Biotechnol 13:868–882

Sun L, Song Y, Qu Y, Yu X, Zhang W (2007) Purification and in vitro cultivation of archaeocytes (stem cells) of the marine sponge Hymeniacidon perleve (Demospongiae). Cell Tissue Res 328:223–237

Valisano L, Pozzolini M, Giovine M, Cerrano C (2012) Biosilica deposition in the marine sponge Petrosia ficiformis (Poiret, 1789): the model of primmorphs reveals time dependence of spiculogenesis. Ancient Animals, New Challenges. Springer, pp. 259–273

Vilanova E, Ciodaro PJ, Bezerra FF, Santos GR, Valle-Delgado JJ, Anselmetti D, Fernàndez-Busquets X, Mourão PA (2020) Adhesion of freshwater sponge cells mediated by carbohydrate–carbohydrate interactions requires low environmental calcium. Glycobiology 30:710–721

Vilanova E, Coutinho C, Maia G, Mourão PA (2010) Sulfated polysaccharides from marine sponges: conspicuous distribution among different cell types and involvement on formation of in vitro cell aggregates. Cell Tissue Res 340:523–531

Wilson H (1907) On some phenomena of coalescence and regeneration in sponges. J Elisha Mitchell Sci Soc 23:161–174

Zhang X, Cao X, Zhang W, Yu X, Jin M (2003) Primmorphs from archaeocytes-dominant cell population of the sponge Hymeniacidon perleve: improved cell proliferation and spiculogenesis. Biotechnol Bioeng 84:583–590